Alma Mater Studiorum – Università di Bologna

DOTTORATO DI RICERCA IN

Scienze Mediche Specialistiche

Ciclo 27

Settore Concorsuale di afferenza: 06/D6

Settore Scientifico disciplinare: MED/26

TITOLO

Multimodal (EEG-fMRI) functional connectivity study of levodopa effect in Parkinson's disease

Presentata dalla Dott.ssa Francesca Pittau

Coordinatore Dottorato	Relatore
Chiar.mo Prof. Roberto Di Bartolomeo	Chiar.mo Prof. Paolo Tinuper

Esame finale anno 2015

ABSTRACT

Aim: To assess if the intake of levodopa in patients with Parkinson's Disease (PD) changes cerebral connectivity, as revealed by simultaneous recording of hemodynamic (functional MRI, or fMRI) and electric (electroencephalogram, EEG) signals. Particularly, we hypothesize that the strongest changes in FC will involve the motor network, which is the most impaired in PD.

Methods: Eight patients with diagnosis of PD "probable", therapy with levodopa exclusively, normal cognitive and affective status, were included. Exclusion criteria were: moderate-severe rest tremor, levodopa induced dyskinesia, evidence of gray or white matter abnormalities on structural MRI. Scalp EEG (64 channels) were acquired inside the scanner (1.5 Tesla) before and after the intake of levodopa. fMRI functional connectivity was computed from four regions of interest: right and left supplementary motor area (SMA) and right and left precentral gyrus (primary motor cortex). Weighted partial directed coherence (w-PDC) was computed in the inverse space after the removal of EEG gradient and cardioballistic artifacts.

Results and discussion: fMRI group analysis shows that the intake of levodopa increases hemodynamic functional connectivity among the SMAs / primary motor cortex and: sensory-motor network itself, attention network and default mode network. w-PDC analysis shows that EEG connectivity among regions of the motor network has the tendency to decrease after the intake the levodopa; furthermore, regions belonging to the DMN have the tendency to increase their outflow toward the rest of the brain. These findings, even if in a small sample of patients, suggest that other resting state physiological functional networks, beyond the motor one, are affected in patients with PD. The behavioral and cognitive tasks corresponding to the affected networks could benefit from the intake of levodopa.

TABLE OF CONTENTS

1. INTRODUCTION

1.1 PARKISNON'S DISEASE

Parkinson's disease (PD) is characterized by asymmetrical Parkinsonism (association of bradykinesia with either hypertonia, resting tremor, or postural instability), progressive worsening, and initial benefit from levodopa. PD is primarily a disease of the elderly, slightly preponderant in males. Its prevalence increases with age from about 0.9% among persons 65 to 69 years old to 5% among persons 80 to 84 years old (de Rijk, Tzourio et al. 1997). Three levels of diagnostic confidence are differentiated: Probable, Possible and Definite. Whereas the first two categories are based on clinical criteria alone, the diagnosis of Definite requires neuropthological confirmation (Gelb, Oliver et al. 1999). Concerning response to treatment, 94-100% of patients whose diagnosis was confirmed by autopsy responded to levodopa (Hughes, Daniel et al. 1993; Louis, Klatka et al. 1997). The impact of this molecule on the course of PD is so important, that a whole issue of the journal "Movement Disorder" (Mov Disord., Jan 2015, Volume 30, Issue 1) has been recently dedicated to this topic.

1.2 FUNCTIONAL CONNECTIVITY

Biswal and colleagues demonstrated for the first time (1995) that brain regions that are functionally related, show temporal correlations in the low frequency component of the hemodynamic signal. Functional interactions between brain regions activity, as measured using electrophysiological or hemodynamic signals, can be characterized in several ways. On the one hand, functional connectivity (FC), the most widely used metrics, measures the statistical dependency between different signals obtained by correlation analysis. However, such strategy does not account for the direction of the information flow and cannot therefore infer causality relationships. On the other hand, effective or directed connectivity investigates directional relationships and aims at describing causal influences. Effective connectivity can be investigated using model-driven techniques such as structural equation modeling

(Tomarken and Waller 2005) and dynamic causal modeling (Friston, Harrison et al. 2003) data-driven techniques such as Granger-causal modeling (Granger 1969), or by recording the response of remote areas to focal stimulation of a given brain region (cortico-cortical evoked potentials; (Keller, Bickel et al. 2011)). Connectivity studies can be applied among a set of predefined relevant brain regions selected by the investigator, between one seed region and the rest of the brain or at the whole brain scale, using the spatial resolution of the recording technique. A detailed description of the various approaches used for measuring connectivity is available in studies comparing them to better understand the specific limitations of each technique (Astolfi, Cincotti et al. 2005; Smith, Miller et al. 2011; Plomp, Quairiaux et al. 2014). The results obtained by such connectivity analysis between all pairs of brain regions can be represented in so-called connectivity matrices. Graph topological analysis is then increasingly applied to reduce the complexity of the data and extract meaningful characteristics of the networks (Bullmore and Sporns 2009).

1.2.a BLOOD OXYGEN LEVEL DEPENDENT (BOLD) SIGNAL AND PHYSIOLOGICAL RESTING STATE NETWORKS

The concept of brain networks originated, and has largely benefited, from the use of resting state functional MRI (fMRI). fMRI detects blood oxygen level dependent (BOLD) signal change reflecting metabolically active brain areas not only in relation to a specific physiologic or pathologic event (Ogawa, Tank et al. 1992), but also in resting state condition (resting state-fMRI or RS-fMRI).

FC detects zones that exhibit correlated BOLD fluctuations and, as a result, belong to the same functional network (Greicius, Krasnow et al. 2003). Studies in monkeys (Shmuel and Leopold 2008) and in humans (Fahoum, Zelmann et al. 2013) suggest that FC is related to neuronal processes.

FC can be measured while the subject is performing a behavioral and cognitive task (task-related FC), or while the subject is not performing any specific task (resting state FC). The RSN that is mainly activated in condition of resting wakefulness and deactivated in task performing is called Default Mode Network (DMN) (Raichle, MacLeod et al. 2001). This physiological RSN is involved in self-referential thoughts and consciousness (Buckner, Andrews-Hanna et al. 2008) (Cavanna and Trimble 2006). The concept of "resting" is debatable (Centeno and Carmichael 2014). Usually subjects are instructed to lie down in the scanner with the eyes closed, and are invited to not sleep.

Different methods have been developed to extract RSNs, some requiring an "a priori hypothesis", like seed-based approach (Biswal, Yetkin et al. 1995), other do not (i.e., independent component analysis (McKeown, Makeig et al. 1998), or bootstrap analysis (Bellec, Rosa-Neto et al. 2010; Dansereau, Bellec et al. 2014)). Methodological aspects of these techniques are available in specific papers (Lemieux, Daunizeau et al. 2011; Biswal 2012; Stefan and Lopes da Silva 2013).

1.2.b ELECTROENCEPHALOGRAPHY (EEG) AND FUNCTIONAL CONNECTIVITY

Functional connectivity algorithms similar to those used for fMRI BOLD signals can be applied to EEG current density estimations in the source space (inverse solution, (Michel, Murray et al. 2004) revealing brain areas that are synchronized in specific frequency bands. As with fMRI, such analysis can be applied to task-related (De Vico Fallani, Astolfi et al. 2010), as well as to spontaneous resting-state activity (de Pasquale, Della Penna et al. 2010; Brookes, Woolrich et al. 2011). The unique advantage of EEG connectivity analysis is the high temporal resolution that allows studying fast fluctuations within large-scale network interactions and fast switches between resting-state networks.

Partial directed coherence (PDC) is a measure in the frequency domain that quantifies to what degree a power change at frequency *f* predicts a power change in another region at *f*.

So, PDC represents a directional rate of change in the spectral power between two regions: large PDC(*f*) indicates that increased spectral power in the source region yields a large increase in the destination region (Schelter, Timmer et al. 2009). However, the PDC calculation is independent of the signal spectral power, and therefore large PDC can occur from regions that show little spectral power, and vice versa. To increase the physiological interpretability, a new method has been developed (Plomp, Quairiaux et al. 2014), consisting in weighting PDC values by the instantaneous power spectral density in the source region. This weighting reflects the fact that activity in a source region is necessary, although not sufficient, in order for the source region to effectively drive activity in other regions.

PDC can be considered as a measure of "effective connectivity", because it gives information about the direction of the signal flow. However, the term "EEG functional connectivity (EEG-FC)" will be used hereunder, both for practical reasons, and in order to use the same terminology that can be found in the literature concerning PDC.

Very few studies compared BOLD-FC and EEG-FC. For this reason, the electrophysiological substrate of spontaneous BOLD fluctuations constituting the basis of FC is still largely unknown. In animal model, the simultaneous fMRI and intracortical neurophysiological recording allowed the detection of correlation between slow fluctuations in BOLD signals and concurrent fluctuations in the underlying locally measured neuronal activity (Logothetis 2012) (Shmuel and Leopold 2008).

Measuring different signals, FC studies performed on invasive EEG recordings can give complementary insight on functional connectivity of brain network. Such studies are ethically feasible for diseases, like epilepsy and PD, which require the implantation of intracranial electrodes.

1.2.c FUNCTIONAL CONNECTIVITY AND PARKISNON'S DISEASE

In the last decades, dysfunctions in the temporal patterning of neuronal discharge have been shown to be involved in the development of parkinsonian symptoms (Marsden and Obeso 1994; Obeso, Rodriguez et al. 1997; Brown and Marsden 1999). Studies in patients undergoing functional neurosurgery suggest the existence of an excessive synchronization of neurons in the subthalamic nucleus (STN) and globus pallidus (Hurtado, Gray et al. 1999; Levy, Hutchison et al. 2000; Levy, Hutchison et al. 2002; Brown 2003) particularly evident in the beta band from 13 to 30 Hz. This synchronization is reduced by treatment with levodopa (Marsden, Werhahn et al. 2000; Brown, Oliviero et al. 2001; Levy, Ashby et al. 2002; Priori, Foffani et al. 2002; Williams, Tijssen et al. 2002). Treatment with levodopa is instead associated with synchronization in the gamma band (Cassidy, Mazzone et al. 2002; Williams, Tijssen et al. 2002; Foffani, Priori et al. 2003). The finding of frequency- and dopaminergic state-dependent coherence between population activity in STN, globus pallidus internus and cerebral cortex suggests that these spectral changes in oscillatory activity are at least in part a network phenomena. With this assumption, abnormal synchronized neuronal activity in the basal ganglia is linearly coupled to activity in the cortex, particularly the motor cortex. Basal ganglia disease leads to motor dysfunctions through effects on its executive motor projection sites, the motor areas of the cerebral cortex and brainstem. Oscillatory synchronization within and between cortical areas is increasingly recognized as a key mechanism in motor organization (Leocani, Toro et al. 1997; Farmer 1998; Gerloff, Richard et al. 1998; Andres, Mima et al. 1999; Ohara, Mima et al. 2001; Serrien and Brown 2002; Serrien and Brown 2003; Serrien, Fisher et al. 2003).

1.3 AIM

The aim of this study is to assess if the administration of levodopa to patients with PD changes cerebral FC, as revealed by simultaneous recording of hemodynamic (fMRI) and by electrical (EEG-PDC) signals. Particularly we hypothesize that the highest changes in FC will involve the motor network, which is the most impaired in PD.

The simultaneous acquisition of EEG and fMRI will allow a better understanding of the relationship between functional fMRI and effective EEG connectivity.

2. METHODS

Between January and December 2012 the EEG-fMRI machinery and competences were settled at the IRCSS Istituto delle Scienze Neurologiche di Bologna (DIBINEM, Dipartimento di Scienze Biomediche e Neuromotorie) (see Appendix).

2.1 SUBJECTS AND EXPERIMENTAL DESIGN

Between January 2013 and May 2013 eight patients were recruited at the IRCSS Istituto delle Scienze Neurologiche di Bologna (DIBINEM, Dipartimento di Scienze Biomediche e Neuromotorie), when meeting the following inclusion criteria: 1) diagnosis of Parkinson's disease "probable" (at least 3 years of disease); 2) L-dopa therapy (other drugs as dopaminergic agents or MAO inhibitors stopped a week before). Exclusion criteria were 1) moderate-severe rest tremor; 2) L-dopa induced dyskinesia; 3) evidence of gray or white matter abnormalities on conventional MRI (i.e. ischemic lesions); 4) contraindications for MR scan (e.g. metallic prosthesis, claustrophobia.). No healthy controls were included, as the goal of the study was to compare connectivity patterns before and after the subministration of L-dopa (i.e. patients themselves without assuming L-dopa are considered as controls). All participants provided written informed consent with a protocol approved by the local Ethics Committee.

Data from two patients had to be discarded: in one case due to particularly strong anxiety and perspiration during the acquisition (leading to strong movement artifacts on MRI and EEG sequences); in the other case the patient didn't manage to undergo the acquisition until the end of the session due to claustrophobia.

Therefore data of six patients (4 male, 2 female) were analyzed. Clinical details are illustrated in Table 1.

N	Age (yrs)	Sex	Age at onset (yrs)	Side of onset	Disease duration (yrs)	HY stage	UPDRS off	UPDRS on	UPDRS reduction after L-dopa (%)
1	46	F	60	R	6	2	19	9	53
2	58	M	55	L	3	2	17	6	65
3	52	F	48	R	4	2	18	10	44
4	46	M	41	R	5	2	17	8	53
5	48	M	54	L	4	2	19	10	48
6	57	M	51	R	6	2	15	10	33
Mean (sd)			51 (6)		5 (1)		17 (1)	9 (2)	49* (10)

Table 1: clinical characteristics of the analyzed patients: (HY: Hoehn and Yahr stating of severity of Parkinson disease, UPDRS: Unifed Parkinson's Disease Rating Scale). UPDRS value significantly reduced after levodopa administration (Wilcoxon test, non-parametric test as samples are not normally distributed $p<0.05$).

2.2 EEG-FMRI ACQUISITION

Brain fMRI acquisitions were performed using a 1.5-T MR medical scanner (GE Medical Systems Signa HDx 15) equipped with a 8-channel phased array brain receiver coil (1.5T HD 8 Channel High Res Head Array for the GE HDx MR System).

The pulse sequence we used for fMRI was a pure axial GR- EPI; for each run, the first five volumes acquired were rejected and slices were acquired in an interleaved way (TR=3000 ms, TE=40 ms, flip angle=90°, number of axial slices per volume=33, number of volumes for run=130, FOV=24 cm, nv=128, voxel dimensions=1.875x1.875x4 mm).

During the functional scan, subjects were asked to lay down without moving and awake with their eyes closed.

A high resolution 3D structural image FSPGR (Fast SPoiled GRadient) with pure axial slices was acquired too (TR=12 ms, TE=5 ms, FOV=25.6 cm, nv=256, voxel dimension=1x1x1 mm).

EEG was recorded simultaneously by using MR compatible equipment (BrainVision, Germany): BrainCap MR (64 channels), BrainAmp MR (amplifier, fiber optic cable and the USB2 Adapter Box), V-Amp (digital DC amplifier with 16 monopolar channels and 2 auxiliary channels). The recording program was BrainVision Recorder and EEG acquisitions were performed with a resolution of $0.1\mu V$ and a sampling frequency of $5kHz$. Pulse (heartbeat) was monitored by ECG recorded at the same sampling frequency by means of a specific ECG cable, as it is useful in removing the cardiac artefact from the EEG trace.

MR compatible cap was placed on the patient's head before the MR scans. Impedences were kept below 5 KOhm.

All patients were scanned twice in the same morning immediately before ('OFF medication' condition) and after ('ON medication' condition) L-dopa administration. To avoid possible systematic effects of circadian origin, all patients were scanned on the same week-day, starting with the first scan at the same day time of the morning.

Each patient was examined firstly before the intake of the first daily dose of L-dopa. He underwent UPDRS (Unified Parkinson's Disease Rating Scale) testing (OFF state - without taking L-dopa). Then the EEG cap was placed by neurophysiopathology technicians and the patient was positioned in the scanner (using fixed landmarks on the head as reference for position).

After a three plane localizer and a calibration sequence, two runs of resting state EEG-fMRI were acquired ($6min45s$ and 130 volumes each) during the OFF state. Then the patient exited the scanner and took L-dopa ($100mg$) and he was tested clinically every $5-10min$ until the start of the L-dopa effect (mean time $30min$) and UPDRS testing was performed, in the ON state.

The patient was repositioned in the scanner (using the previous landmarks) and two runs of resting state were acquired (6*min*45*s* each one, 130 volumes) during the ON state, with the same technical parameters as the acquisition during the OFF state.

Finally, the high-resolution 3D structural image was acquired, during the ON state, when the patient was still wearing the EEG cap.

2.3 EEG-FMRI DATA PROCESSING AND ANALYSIS

2.3.A FMRI

fMRI data pre- processing and processing have been performed using software tools within FSL (FMRIB's software Library, FMRIB, Oxford, Uk, *http://fsl.fmrib.ox.ac.uk/fsl/* version 4.1.4, (Jenkinson, Beckmann et al. 2012), and within AFNI (*AFNI: http://afni.nimh.nih.gov/afni/* version AFNI_2008_07_18_1710, (Cox 1996)). Functional data preprocessing after physiological noise correction of raw data, was carried out using FSL tools. A high pass filter cut off set at 100s, the motion correction by the tool of FSL, MCFLIRT, the slice timing correction (interleaved), the brain extraction by BET, the spatial smoothing performed with a Gaussian filter of FWHM 6mm, the FILM prewhitening and the estimation of head motion parameters which were added as confounding variables in the model.

To perform functional connectivity analyses we defined two regions of interest (ROI): the supplementary motor area - SMA (right and left) and the precentral gyrus (right and left) (M1 - primary motor area); SMA is critical in initiating movements, whereas bilateral M1 are critical in motor execution.

The seeds were drawn manually by a neurologist (R.G.) in the MNI space, as spheres centered in the coordinates reported in Table 2 and with a radius of 5mm.

seed	x	y	z
R-PG (right precentral gyrus)	23 (44.00)	59 (-8.00)	55 (38.00)
L-PG (left precentral gyrus)	67 (-44.00)	59 (-8.00)	55 (38.00)
R-SMA (right SMA)	42 (6.00)	63 (0.00)	63 (54.00)
L-SMA (left SMA)	48 (-6.00)	63 (0.00)	63 (54.00)

Table 2: Coordinates (in MNI standard space, voxels (mm)) of spherical seed's centres)

For the first-level analysis the GLM was performed considering as regressor the averaged time series of each seed. Z statistic images were thresholded using clusters determined by Z = 2.3 and a family-wise-error corrected cluster significance threshold of p = 0.05 was applied to the suprathreshold clusters.

Functional data were aligned to structural images (within-subject) initially using linear registration (FMRIB's Linear Image Registration Tool, FLIRT). Structural images were transformed to standard space using a non-linear registration tool (FNIRT), and the resulting warp fields applied to the functional statistical summary images.

The second level (within-subject analysis or between-session analysis) fixed effects analysis combined the data of the two resting state runs in the OFF-state and two runs in the ON-state, obtaining each subject's mean response.

The third-level analysis was the group statistical analysis. We used a mixed-effects regression model in order to model the subject. A Paired Two-Group Difference (Two-Sample Paired T-Test) was performed to compare the two groups. We compared, for the same group of patients, activations and deactivations in the connectivity with each of the four seeds, before (OFF state) and after (ON state) the assumption of L-dopa.

Finally, the z-statistic images were thresholded and underwent a clustering analysis. The contrasts were performed both for OFF versus ON and ON versus OFF.

To quantify the significant variation in connectivity with the seeds, brain areas showing increased connectivity were defined on the basis of AAL atlas (Tzourio-Mazoyer, Landeau et al. 2002), Broadman areas were identified according to the overlapping between AAL areas and Broadman areas as defined in in an atlas included in WFU Pickatlas 3.0.4 (Lancaster, Woldorff et al. 2000; Maldjian, Laurienti et al. 2003).

We did not explore whether the variations of brain connectivity correlate with the disease severity because of the homogeneity of the UPDRS motor score in the OFF state.

2.3.b EEG

Patients underwent 63 channels EEG recording (reference electrode Cz). Brain Vision Analyser software (Brain Products, Munich, Germany) was used for off-line correction of the gradient artifact and filtering of the EEG signal (Allen, Josephs et al. 2000). A 50-Hz low-pass filter was also applied to remove the remaining artifact. The ballistocardiogram artifact and eye-movements and blinking artifacts were removed by independent component analysis (Benar, Aghakhani et al. 2003). Then, EEG signals were down-sampled to 250 Hz. The so obtained EEG signals, both in OFF period and ON period, were examined by visual inspection to remove sections containing muscular artifacts and sleep patterns. In both condition, the artifact-free sections were concatenated.

2.3.b.1 REGIONAL ELECTRICAL SOURCE IMAGING (ESI)

The forward model consisted in a simplified realistic head model with consideration of skull thickness (Locally Spherical Model with Anatomical Constraints [LSMAC] (Birot, Spinelli et al. 2014; Megevand, Spinelli et al. 2014)). From a template MNI brain MRI, around 5,000 solution-points were distributed equally in the gray matter, which represented the solution space. A linear distributed inverse solution with biophysical constraints was used to calculate

the three-dimensional (3D) current density distribution (Local Auto-Regressive Averages [LAURA]), (Grave de Peralta Menendez, Murray et al. 2004). The brain was parcelled into 82 regions of interest (ROIs) using the automated anatomic labeling (AAL) digital atlas (Tzourio-Mazoyer, Landeau et al. 2002) coregistered with the MNI brain using the inverse segmentation matrix obtained in SPM8 (www.fil.ion.ucl.ac. uk/spm).

2.3.b.2 WEIGHTED PARTIAL DIRECTED COHERENCE

For each patient we calculated the power spectral density (PSD) using the Fast Fourier Transform (FFT). The PDC results (for both ON and OFF epochs) were analyzed for each frequency band. To determine the PSD for each voxel in the inverse space, FFT was computed for each scalp electrode, and source estimation was then applied to this frequency-domain complex data. The mean PSD for each patient was computed and normalized (0–1) across regions and frequencies (1–40 Hz) by subtracting the minimum power and dividing by the range. PDC was computed using a multivariate autoregressive model (MVAR) of order 10. PDC is defined in terms of MVAR coefficients transformed to the frequency domain. In this study, PDC values were scaled (in the same way as the ST) and multiplied by the spectral power (weighted PDC, wPDC). A full description of the wPDC method used can be found in previous work (Plomp, Quairiaux et al. 2014; Coito, Plomp et al. 2015). For each subject, we computed the wPDC for each epoch and frequency. We analyzed then the average wPDC for each subject in 3 frequency bands: theta (4-8 Hz), alpha (8-12 Hz) and beta (12-30 Hz). For each of these bands, we computed the summed outflow (Coito et al, 2015). We then assessed the whole-brain connectivity from each region. For specifically investigating the motor cortex interactions, we analysed the connectivity results only in between the left and right precentral gyrus and SMA regions. For each patient, the summed outflow of each region at each time point of the OFF segments was compared to each time point of the ON segments with a nonparametric test (Mann-Whitney-Wilcoxon, $p < 0.05$). EEG and ESI analysis were carried out using the freely available software Cartool (brainmapping.unige.ch/cartool) and Matlab

(MATLAB and Statistics Toolbox Release 2012b, The MathWorks, Inc., Natick, Massachusetts, United States). For some figures, we used a modified version of the e-connectome toolbox (He, Dai et al. 2011).

3. RESULTS

3.1 FMRI

A statistically significant increased connectivity with all four seeds was found for the contrast ON vs. OFF state with different extent and within different areas. Figure1 shows group analysis results, overlapped to the MNI template.

The connectivity areas that showed a positive significant difference between ON state and OFF state, averaging all 6 patients, are displayed in hot color. Figure 1 box R-PG refers to connectivity with right precentral gyrus, Figure 1 box L-PG with left precentral gyrus, Figure 1 box R-SMA with right SMA and Figure 1 box L-SMA with left SMA. Images show sagittal views of the main areas in which we found significant clusters of voxels.

In details, the brain areas showing significantly stronger connectivity with the four seeds for the contrast ON vs. OFF states are reported in Table 3-6.

Conversely, the group analysis showed no significant variations in connectivity for the contrast OFF state vs. ON state, thus there are no brain areas in which the connectivity with the four seeds significantly decreased after the intake of L-dopa.

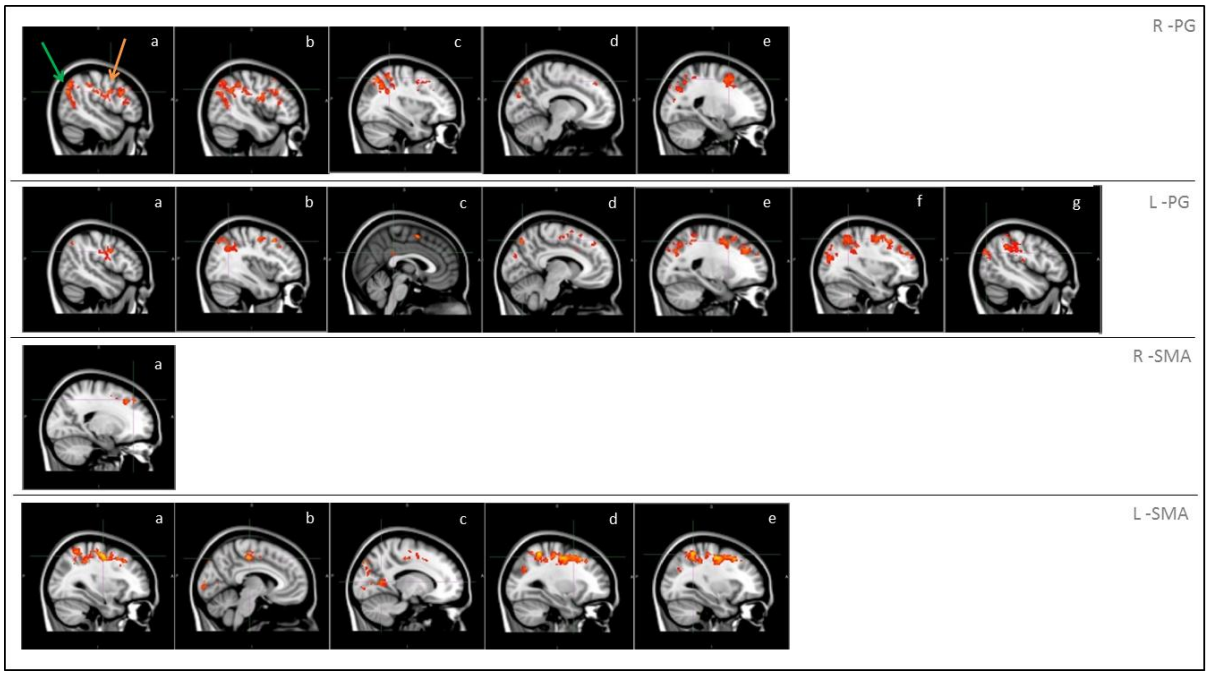

Figure 1 – Functional connectivity in the group analysis of ON state vs. OFF state; box R-PG connectivity with seed in right precentral gyrus (a: occipital cortex -green arrow-, motor areas -orange arrow-, b: angular gyrus, c: superior parietal lobe, d: precuneus, e: superior frontal gyrus);

box L-PG connectivity with seed in left precentral gyrus (a: motor areas, d: angular gyrus, f: cingulum, e: precuneus, b: superior frontal gyrus, c: superior parietal lobe, g: occipital cortex); box R-SMA connectivity with seed in right SMA (a: frontal pole – superior frontal gyrus); box L-SMA connectivity with seed in left SMA (a,b : motor areas, c: precuneus, d: middle/superior frontal gyrus, e: superior parietal lobe).

BRAIN AREAS	BRODMANN AREAS	VOXELS	MAX INTENSITY	COORDINATES MAXIMUM VOXEL		
				x	y	z
Angular gyrus L	39, 19, 22	72	2.83	66	39	53
Angular gyrus R	39, 19, 22	685	3.29	25	31	60
Middle Cingulate L	31, 32, 23, 24	0	0.00	0	0	0
Middle Cingulate R	31, 32, 23, 24	13	2.57	41	39	52
Posterior Cingulate L	31, 23, 118	0	0.00	0	0	0
Posterior Cingulate R	31, 23, 118	40	3.01	40	43	49
Middle Frontal L	6, 8, 9, 10	259	2.88	56	65	60
Middle Frontal R	6, 8, 9, 10	211	3.04	22	74	53
Superior Frontal L	6, 8, 9, 10	132	2.97	55	69	61
Superior Frontal R	6, 8, 9, 10	257	2.91	33	74	59
Superior Occipital L	18, 19, 7, 31	187	2.98	53	20	48
Superior Occipital R	18, 19, 7, 31	53	2.81	32	28	58
Superior Parietal L	7, 19	167	2.91	59	36	61
Superior Parietal R	7, 19	115	2.95	28	31	61
Postcentral gyrus L	1, 2, 3, 40, 43	201	2.90	73	57	57
Postcentral gyrus R	1, 2, 3, 40, 43	121	2.93	12	59	47
Precentral gyrus L	3, 4, 6	15	2.54	59	64	60
Precentral gyrus R	3, 4, 6	61	3.05	22	63	50
Precuneus L	31, 7, 23, 29	57	2.79	50	28	61
Precuneus R	31, 7, 23, 29	141	2.85	39	34	56
SMA L	6	18	2.81	46	75	60
SMA R	6	1	2.33	39	75	59

Table 3. List of main brain areas showing a significant variation in connectivity with the right precentral gyrus when comparing the ON state versus the OFF state (z-statistic map, from a 2 samples paired t-test, $p < 0.05$, cluster correction). Coordinates are given in voxels, referred to the MNI space. Brain areas were defined on the basis of AAL atlas (N. Tzourio-Mazoyer 2002), Broadman areas were identified according to the overlapping between AAL areas and Broadman areas as defined in in an atlas included in WFU Pickatlas 3.0.4.

BRAIN AREAS	BRODMANN AREAS	VOXELS	MAX INTENSITY	COORDINATES MAXIMUM VOXEL		
				x	y	z
Angular gyrus L	39, 19, 22	33	2.860074	68	24	51
Angular gyrus R	39, 19, 22	195	2.970902	25	31	60
Middle Cingulate L	23, 24, 31, 32	7	2.498789	49	70	54
Middle Cingulate R	23, 24, 31, 32	3	2.455251	42	46	51
Posterior Cingulate L	23, 31, 118	4	2.739749	44	45	50
Posterior Cingulate R	23, 31, 118	23	2.911491	41	44	50
Middle Frontal L	6, 8, 9, 10	696	3.287124	59	69	64
Middle Frontal R	6, 8, 9, 10	361	3.309958	25	72	60
Superior Frontal L	6, 8, 9, 10	413	3.198812	58	81	54
Superior Frontal R	6, 8, 9, 10	356	3.050314	36	75	64
Superior Occipital L	18, 19, 7, 31	130	3.037495	57	26	54
Superior Occipital R	18, 19, 7, 31	39	2.913447	29	26	58
Superior Parietal L	7, 19	207	2.896308	53	29	63
Superior Parietal R	7, 19	17	2.772044	31	25	60
Postcentral gyrus L	2, 3, 40, 43	235	2.863164	72	56	56
Postcentral gyrus R	2, 3, 40, 43	134	3.112937	13	60	50
Precentral gyrus L	3, 4, 6	154	2.988253	61	63	64
Precentral gyrus R	3, 4, 6	264	3.078538	29	59	63
Precuneus L	7, 31, 23, 29	59	2.95629	49	26	60
Precuneus R	7, 31, 23, 29	6	2.347032	35	25	59
SMA L	6	150	3.299979	45	64	64
SMA R	6	58	3.252035	44	64	64

Table 4. List of main brain areas showing a significant variation in connectivity with the left precentral gyrus when comparing the ON state versus the OFF state (z-statistic map, from a 2 samples paired t-test, $p < 0.05$, cluster correction).

BRAIN AREAS	BRODMANN AREAS	VOXELS	MAX INTENSITY	COORDINATES MAXIMUM VOXEL		
				x	y	z
Angular gyrus L	39, 19, 22	0	0	0	0	0
Angular gyrus R	39, 19, 22	0	0	0	0	0
Middle Cingulate L	23, 24, 31, 32	0	0	0	0	0
Middle Cingulate R	23, 24, 31, 32	0	0	0	0	0
Posterior Cingulate L	23, 31, 118	0	0	0	0	0
Posterior Cingulate R	23, 31, 118	0	0	0	0	0
Middle Frontal L	6, 8, 9, 10	0	0	0	0	0
Middle Frontal R	6, 8, 9, 10	363	3.09	25	72	58
Superior Frontal L	6, 8, 9, 10	0	0	0	0	0
Superior Frontal R	6, 8, 9, 10	158	2.99	36	77	57
Superior Occipital L	18, 19, 7, 31	0	0	0	0	0
Superior Occipital R	18, 19, 7, 31	0	0	0	0	0
Superior Parietal L	7, 19	0	0	0	0	0
Superior Parietal R	7, 19	0	0	0	0	0
Postcentral gyrus L	2, 3, 40, 43	0	0	0	0	0
Postcentral gyrus R	2, 3, 40, 43	0	0	0	0	0
Precentral gyrus L	3, 4, 6	0	0	0	0	0
Precentral gyrus R	3, 4, 6	11	2.61	26	64	61
Precuneus L	7, 31, 23, 29	0	0	0	0	0
Precuneus R	7, 31, 23, 29	0	0	0	0	0
SMA L	6	0	0	0	0	0
SMA R	6	0	0	0	0	0

Table 5. List of main brain areas showing a significant variation in connectivity with the right supplementary motor area when comparing the ON state versus the OFF state (z-statistic map, from a 2 samples paired t-test, $p < 0.05$, cluster correction.

BRAIN AREAS	BRODMANN AREAS	VOXELS	MAX INTENSITY	COORDINATES MAXIMUM VOXEL		
				x	y	z
Angular gyrus L	39, 19, 22	0	0	0	0	0
Angular gyrus R	39, 19, 22	51	2.80	26	34	54
Middle Cingulate L	23, 24, 31, 32	78	3.19	48	51	60
Middle Cingulate R	23, 24, 31, 32	31	2.60	38	55	61
Posterior Cingulate L	23, 31, 118	0	0	0	0	0
Posterior Cingulate R	23, 31, 118	5	2.63	40	44	50
Middle Frontal L	6, 8, 9, 10	469	3.36	62	72	60
Middle Frontal R	6, 8, 9, 10	398	3.32	33	75	57
Superior Frontal L	6, 8, 9, 10	196	3.12	56	61	63
Superior Frontal R	6, 8, 9, 10	233	3.24	33	74	57
Superior Occipital L	18, 19, 7, 31	144	3.07	51	23	47
Superior Occipital R	18, 19, 7, 31	0	0	0	0	0
Superior Parietal L	7, 19	162	3.35	60	39	64
Superior Parietal R	7, 19	191	3.12	31	37	64
Postcentral gyrus L	2, 3, 40, 43	373	3.23	68	47	63
Postcentral gyrus R	2, 3, 40, 43	164	3.19	32	38	63
Precentral gyrus L	3, 4, 6	370	3.38	61	58	61
Precentral gyrus R	3, 4, 6	250	3.46	29	59	61
Precuneus L	7, 31, 23, 29	8	2.46	53	35	43
Precuneus R	7, 31, 23, 29	62	2.81	38	36	54
SMA L	6	57	2.88	46	62	63
SMA R	6	97	2.84	39	52	64

Table 6. List of main brain areas showing a significant variation in connectivity with the left supplementary motor area when comparing the ON state versus the OFF state (z-statistic map, from a 2 samples paired t-test, $p < 0.05$, cluster correction).

3.2 EEG

By calculating the connections among the 4 seeds of the motor system (right and left pre-central gyri; right and left SMA) we did not find any significant difference in PDC in ON vs. OFF ($p>0.05$) for all the studied frequencies (alpha, beta, theta) (figures 2, 3, 4). Although not significant, a trend toward a decreased FC in ON vs. OFF among the different structures of the motor system can be observed, for each frequency.

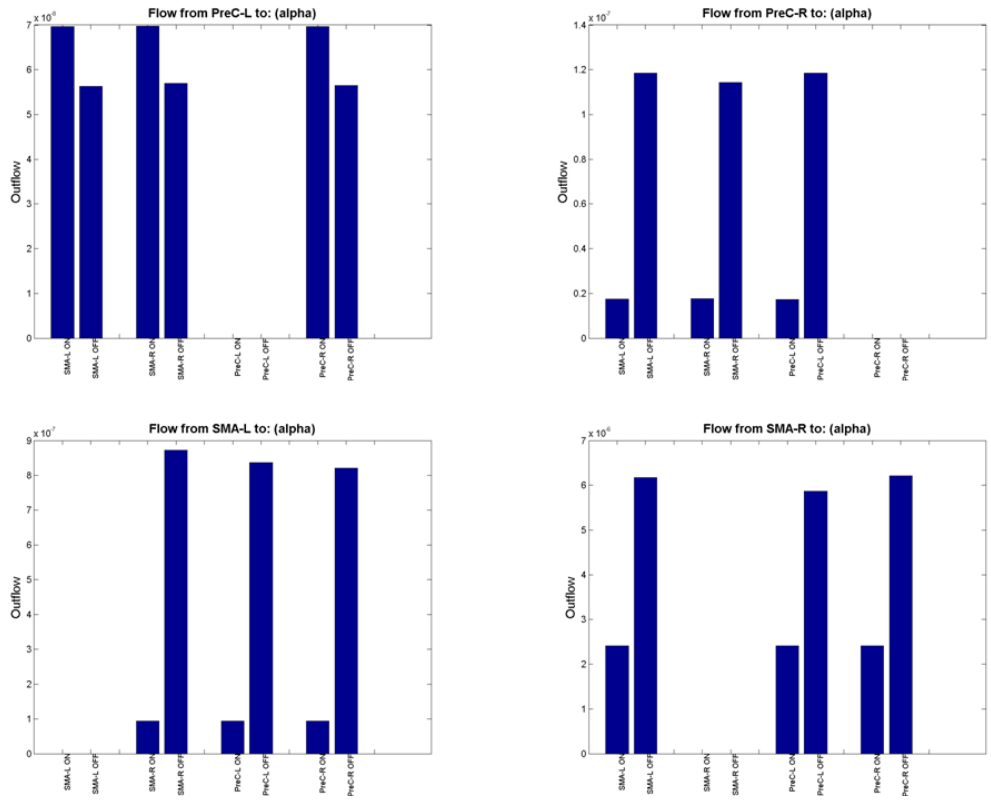

Figure 2: connections among right and left pre-central gyri and right and left SMA in the apha band

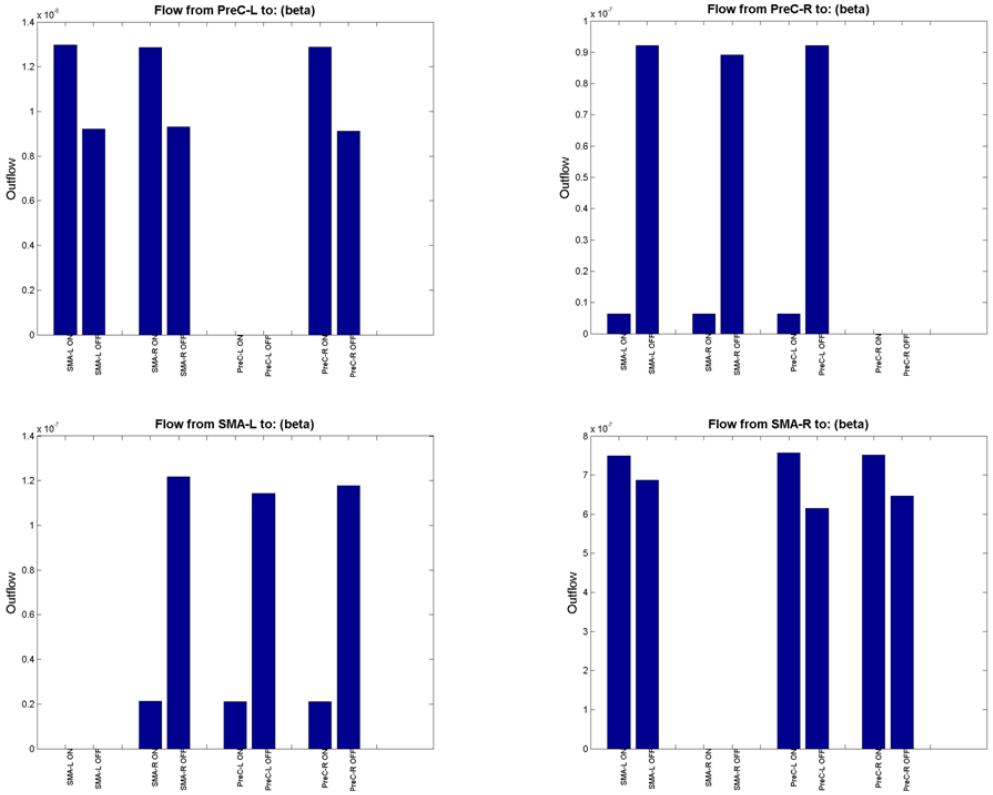

Figure 3: connections among right and left pre-central gyri and right and left SMA in the beta band

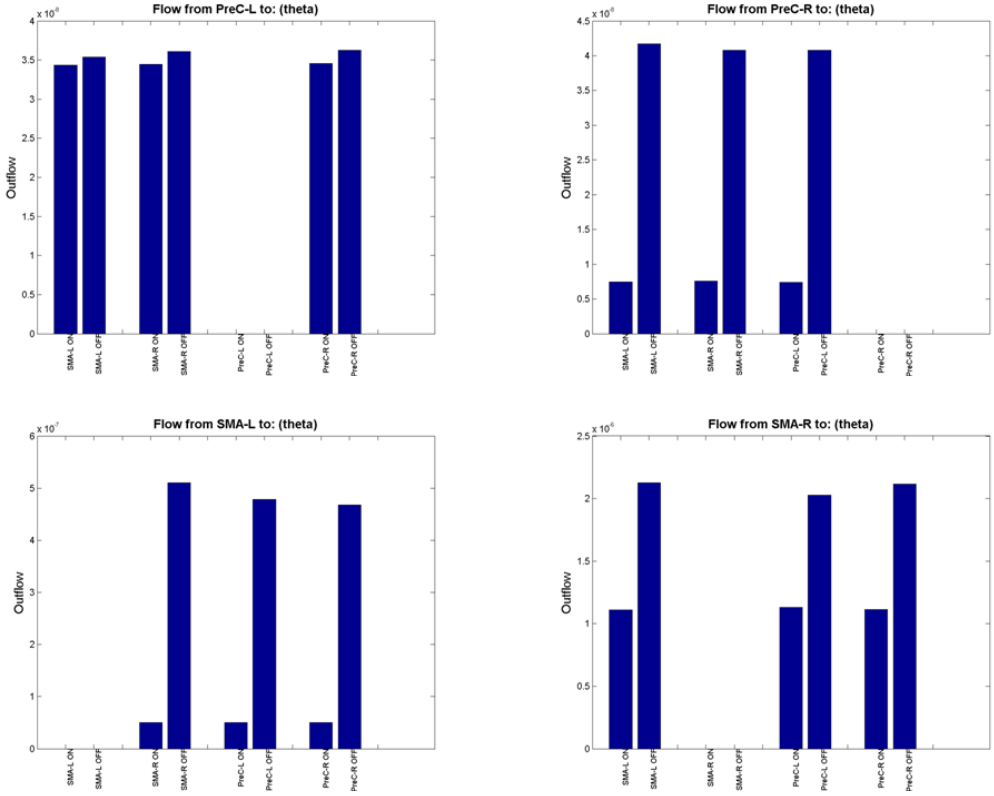

Figure 4: connections among right and left pre-central gyri and right and left SMA in the theta band

We calculated if the motor system was augmenting its outflow, in On vs. OFF, toward the rest of the brain. We did not find any significant difference (figure 5) for any considered frequency ($p>0.05$). As before, we can observe a tendency toward a decreased summed outflow from the motor system, especially concerning the alpha and the theta bands.

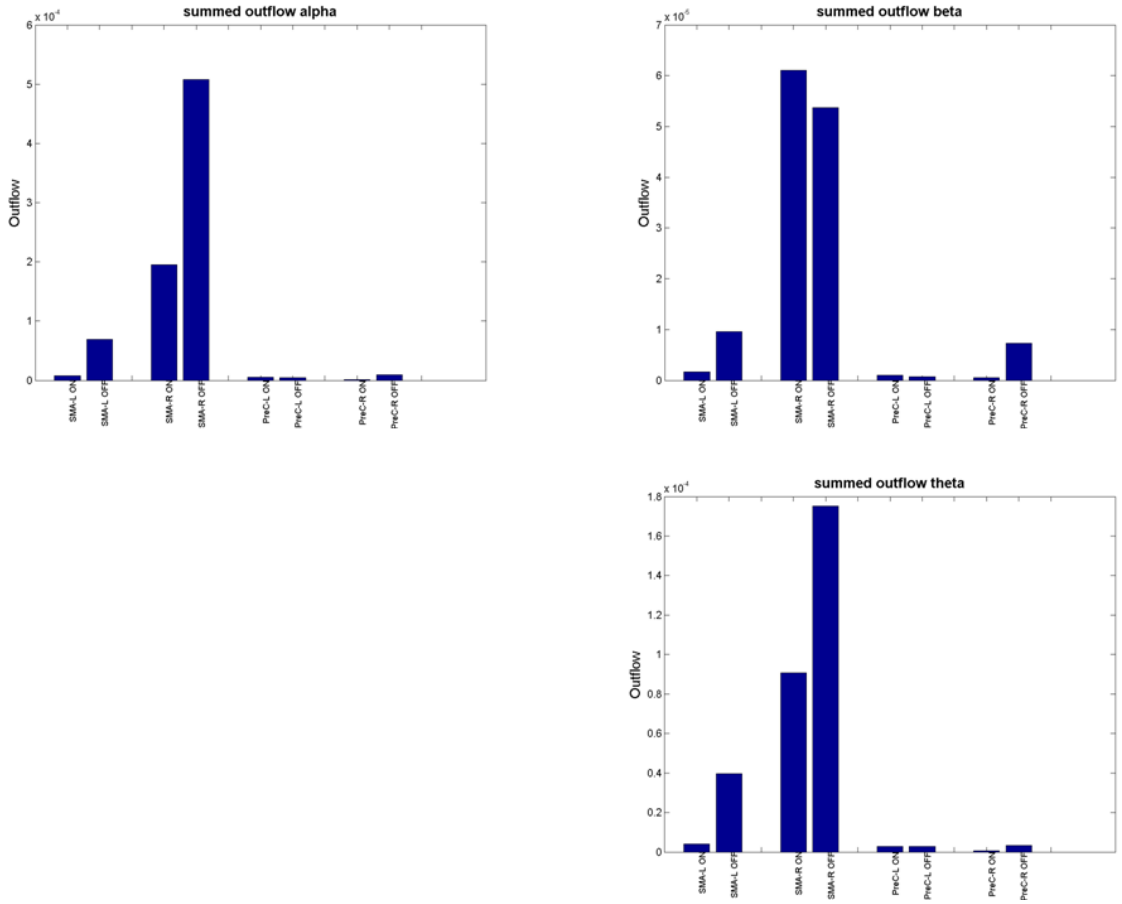

Figure 5: summed outflow from the 4 ROIs in ON and in OFF in the alpha, beta and theta band

When we performed the PDC from each ROI of the whole brain, the only structures who showed a strong tendency ($p<0.06$) in changing their summed outflow in ON vs. OFF are represented in figures 6, 7, and 8. They belong essentially to the DMN.

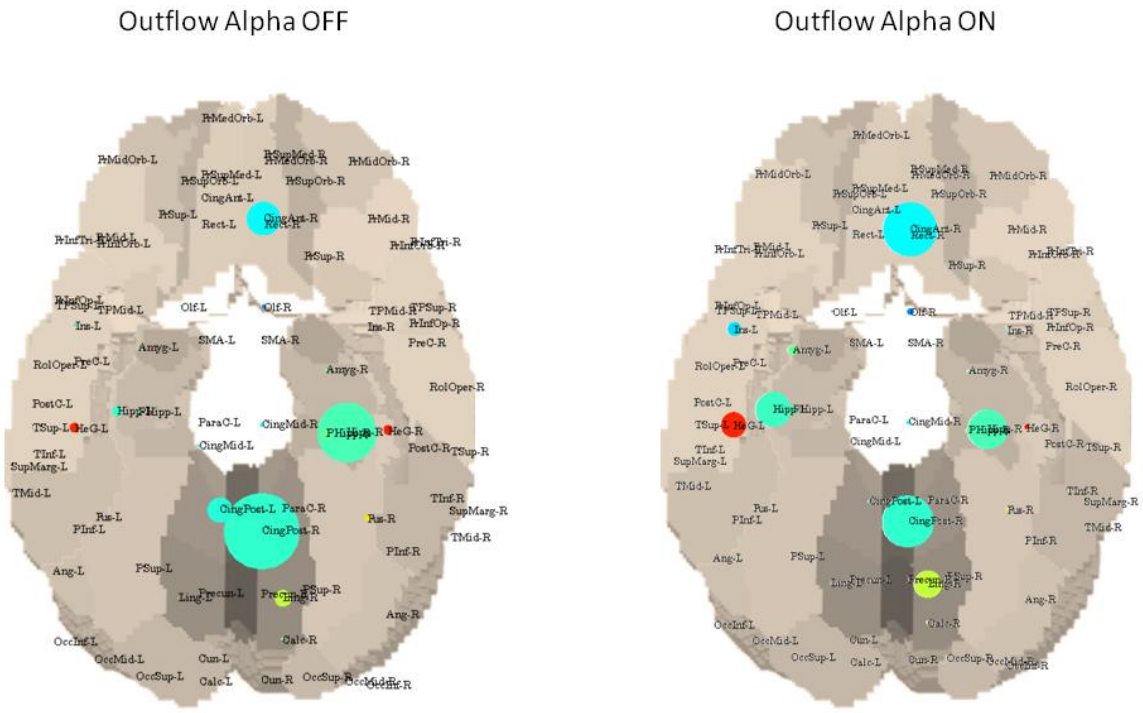

Figure 6: On the left: outflow for each ROI in the alpha band, in OFF. On the right: same representation in ON. Regions showing a strong tendency to change their outflow in ON vs. OFF are: posterior cingulates, left amygdala and hippocampus, right anterior cingulate, right lingual gyrus.

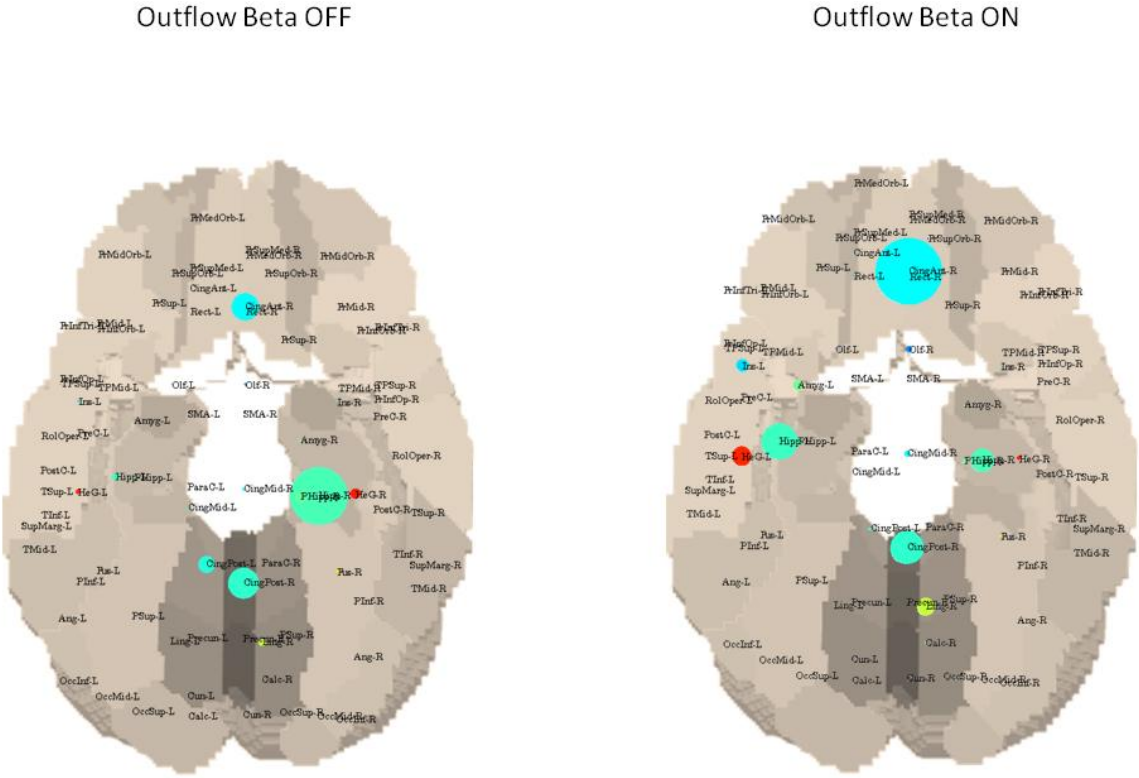

Figure 7: On the left: outflow for each ROI in the beta band, in OFF. On the right: same representation in ON. Regions showing a strong tendency to change their outflow in ON vs. OFF are: left amygdale, bilateral hippocampi, and right anterior cingulate.

Outflow Theta OFF

Outflow Theta ON

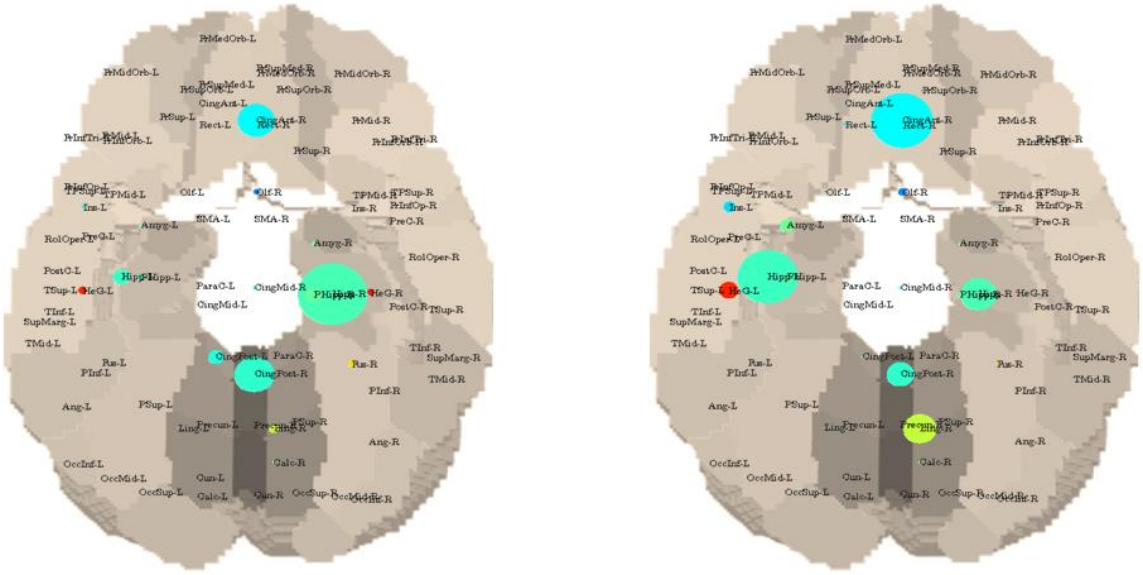

Figure 8: On the left: outflow for each ROI in the theta band, in OFF. On the right: same representation in ON. Regions showing a strong tendency to change their outflow in ON vs. OFF are: posterior cingulate, left amygdale, bilateral hippocampi, and right anterior cingulate.

Whereas in OFF the strongest connections originate from the posterior regions of the DMN, in ON they come from the anterior cingulated region, another region of the DMN. However, this difference was not statistically significant (figures 9, 10, 11).

Connections alpha OFF

Connections alpha ON

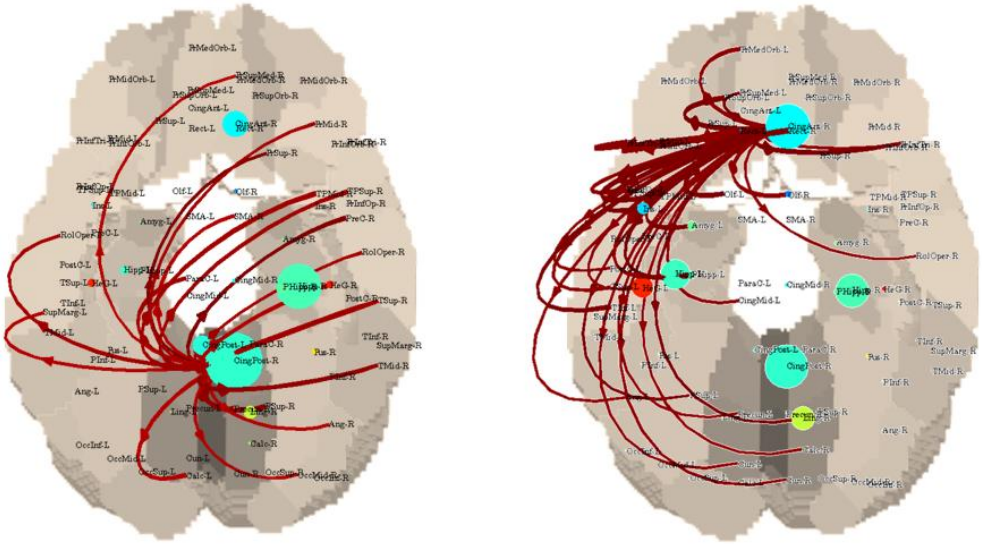

Figure 9: On the left: connection between each ROI in the alpha band, in OFF. On the right: same representation in ON. In the OFF phase the main driver of connections is the posterior cingulate. In ON is the anterior cingulate. Only the strongest 30% connections are shown.

Connections beta OFF

Connections beta ON

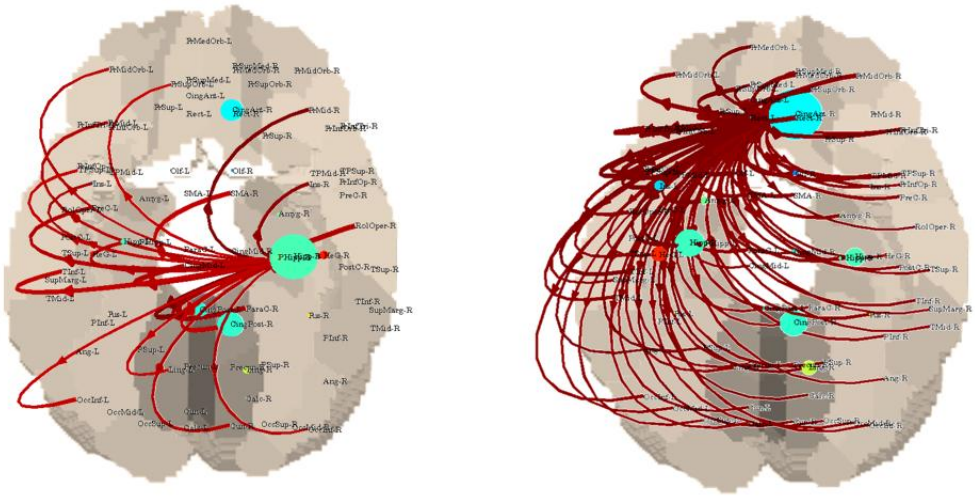

Figure 10: On the left: connection between each ROI in the beta band, in OFF. On the right: same representation in ON. In the OFF phase the main driver of connections is the right hippocampus. In ON is the anterior cingulate. Only the strongest 30% connections are shown.

Connections theta OFF

Connections theta ON

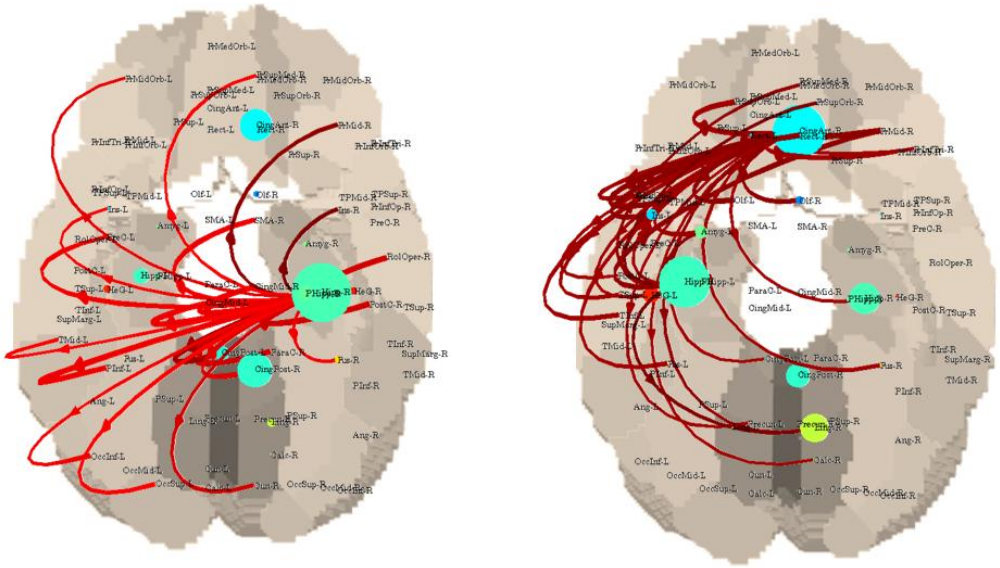

Figure 11: On the left: connection between each ROI in the theta band, in OFF. On the right: same representation in ON. In the OFF phase the main driver of connections is the right hippocampus. In ON is the anterior cingulate. Only the strongest 30% connections are shown.

4. DISCUSSION

This is to our best knowledge, the first study that aimed to assess the effect of levodopa in a population of patients with PD, through resting state functional connectivity measured simultaneously with EEG and fMRI.

FMRI FC

Concerning fMRI data, an increased connectivity with all four seeds, with different extent and within different areas after the intake of L-dopa, can be identified as a general trend.

Main areas connected with the right precentral gyrus presenting an increased FC in ON vs. OFF are: i) the cingulate gyrus (both anterior and posterior) and the precuneus, which are areas involved in the default mode network (DMN), ii) the parietal and occipital areas, involved in attentional and visuo-spatial activities, iii) the dorsal lateral prefrontal cortex (bilateral) and the superior frontal gyrus, related to performance monitoring and executive functions, iv) motor and sensorimotor areas, such as the precentral gyrus, the postcentral gyrus, and the SMA, involved in motor initiation.

Left precentral gyrus and L SMA showed the same increased connectivity in ON vs. OFF as the right precentral gyrus, although with fewer significant voxels.

However, when the seed was placed in the R-SMA there was a smaller number of voxels showing significant differences between ON and OFF, all belonging to the sensory-motor network.

Brain areas that were more involved (i.e. connected with the seeds in primary and supplementary motor cortex) during the ON state rather than the OFF state may be ascribable essentially to three brain networks: the sensorimotor itself, the dorsal-attention and the default mode.

The sensorimotor network deals with the integration of sensitive and motor stimuli, and has been shown to have characteristic activation in pre- and post-central gyri extending from the superior bank of the Sylvian fissure to the medial wall of the interhemispheric fissure, including the SMA (Beckmann, DeLuca et al. 2005). The dorsal attention system, observed for the first time during resting state by Fox and colleagues (Fox, Corbetta et al. 2006) is involved in voluntary orientation and attention. It is mainly represented by the following areas: the Intraparietal sulcus (IPS) and the Frontal Eye Field (FEF), junction of the precentral and superior frontal sulcus. The default mode network is described as the collection of brain structures that are particularly active during rest and deactivated when specific goal-directed behaviour is needed (Damoiseaux, Rombouts et al. 2006). Core regions associated with the brain's default network are the ventral medial prefrontal cortex, the posterior cingulate/retosplenial cortex, the inferior parietal lobule, the lateral temporal cortex, the dorsal medial prefrontal cortex, and according to some authors, the hippocampal formation (Buckner, Andrews-Hanna et al. 2008). This network is active when retrieving and processing past autobiographical events (Greicius, Krasnow et al. 2003).

DMN

The increased connection between motor network and DMN areas after the intake of L-dopa may be due to the fact that patients were more relaxed, and more ready to prepare and perform movements. In a recent Voxel Based Morphometry and fMRI study on cognitively unimpaired PD (Tessitore, Esposito et al. 2012) it has been shown that PD patients, compared to controls, showed a decreased functional connectivity within the DMN (right medial temporal lobe and bilateral inferior parietal cortex). This impairment was not correlated with the total levodopa equivalent daily dose. Nevertheless, it has benne demonstrated (Krajcovicova, Mikl et al. 2012) that dopaminergic therapy has a specific effect on both the DMN integrity and task-related brain activations in cognitively unimpaired PD patients, and that these effects seem to be dose-dependent; this may be consistent with the fact that the

posterior cingulate cortex appears to be more connected with M1 and supplementary motor area after L-dopa intake, as an improvement towards motor preparation and execution. Furthermore there were no differences in DMN integrity between PD on dopaminergic medication and healthy controls, suggesting therefore that dopaminergic therapy may have specific effects on default mode integrity, helping to relatively normalize activation within DMN in PD patients.

Attention network

A notable aspect of our results is that many structures of attentive and executive networks are more connected with primary and supplementary motor areas after the intake of L-dopa, suggesting that dopaminergic medication may help PD patients with their executive dysfunction, giving them notable improvements in the cognitive, attentional and executive steps, essential in the phase of preparation of a movement. Therefore medication with L-dopa also seems to have positive effects during rest, and not only during the performance of movements.

In a study by Tessitore et al., (Tessitore, Amboni et al. 2012) attentional network in PD patients with and without freezing (typical PD symptom, consisting in a sort of motor block due to a visible obstacle, thus related to visual perception) were analysed, founding a reduced activity in patients with freezing. Usually this symptom is not present at the early stage of the disease and none of our patients presented this problems; later it is typically more present when the patients are without medication. From our results we could hypothesize that freezing may be related to a dysfunction of the visuo-spatial network (related to the attentional areas, involving mainly the posterior parietal cortex and middle/inferior frontal gyrus, Table 3 and Table 4), present even before the problem manifests itself. Prospective longitudinal studies could confirm our hypothesis.

One of the first fMRI study on PD (Rowe, Stephan et al. 2002) investigated activations and connectivity during the performance of tasks (a paced overlearned motor sequence task,

with and without an additional attention task): motor and attentional structures were found to be primarily involved. Specifically, only in control subjects, and not in PD patients, an attentional modulation of connectivity was observed: the attention to action leads to further activations of prefrontal, parietal, para-cingulate cortex and SMA. The engagement of the attentional control network in PD was recently investigated (Shine, Halliday et al. 2014): a decreased activation of frontal and parietal hubs of the dorsal attention network were found, supporting the hypothesis that visual misperceptions sometimes found in PD, may arise from disrupted processing across attentional networks.

Sensorymotor network

In our study the intake of L-dopa increases the functional connections of posterior cingulate cortex and precuneus with sensorimotor system. This finding is in agreement with what found by van Eimeren and colleagues (van Eimeren, Monchi et al. 2009). They investigated dysfunctions of the default mode in PD patients and found deficits in executive tasks, which include planning and set shifting, observing less deactivation of posterior cingulate cortex and precuneus. This suggests an impairment of the DMN during executive task in PD patients. Similarly, Esposito and colleaugues (Esposito, Tessitore et al. 2013) studied functional connectivity changes within the sensorimotor resting state network in drug-naive PD patients after acute levodopa administration. They showed that levodopa enhanced the sensorimotor network functional connectivity in the supplementary motor area (where drug-naive patients exhibited reduced signal fluctuations) and that, at the spectral frequency level, levodopa stimulated these fluctuations in a selective frequency band of the sensorimotor network. They did not observe any compensatory effects in other regions of sensorimotor network, assuming that maybe the compensatory effects may arise only during motor performance and not in resting state.

EEG-fMRI is a method that explores the complementary strengths of these tools, which are, the high temporal resolution of EEG and the high spatial resolution of fMRI. The directed connectivity was quantified by calculating the PDC from EEG signals. This study represents the first application of PDC analysis in the EEG acquired inside the fMRI for a clinical purpose.

We were not able to confirm our "a priori hypothesis", i.e. regions belonging to the motor network change their EEG coherence in the ON vs. OFF phase, while the patient is in resting state. Nevertheless, our results suggest some interesting trends, although they are not statistical significant. The first is that in ON the FC among the 4 seeds in the motor system is decreased when compared to the OFF phase. A previous resting state scalp EEG study (Silberstein, Pogosyan et al. 2005) showed that the coherence between C3 and C4 over 10–35 Hz correlated with the severity of parkinsonism, and this cortical coupling was decreased by both L-dopa and subthalamic nucleus (STN) stimulation (linked to clinical improvement). Our results, although not statistical significant, show the same tendency toward a decreased coherence after the intake of levodopa. In the literature the effect of levodopa on coherence is still debated: indeed recent studies could not confirm this effect of pharmacological intervention on cortical coherence. Litvak and colleagues (Litvak, Jha et al. 2011) used magnetoencephalography (MEG) and subthalamic local field potential recordings, to investigate resting connectivity in PD patients, the main findings being relative to the attentional and execution functions. He observed two major spatio-temporal patterns of coupling between the cerebral cortex and subthalamic nuclei: one in the alpha frequency band and one in the beta frequency band. The former showed coherence between subthalamic area and bilateral temporo-parietal cortex and brainstem, and is therefore likely to have an attentional role. The latter involved the subthalamic area and ipsilateral anterior parietal and

frontal cortices, and is likely to be involved in setting executive functions. Interestingly, in this study dopaminergic medication increased this beta coherence between subthalamic regions and the prefrontal cortex. Lalo and colleagues (Lalo, Thobois et al. 2008) investigated the direct transfer function between STN and cortex at rest and during movement, with and without pharmacological dopaminergic input. The authors simultaneously recorded scalp electroencephalographic activity and local field potentials from depth electrodes across several frequency bands: also in this study the coherence in the beta band did not change after dopaminergic therapy. Pollok and colleagues (Pollok, Kamp et al. 2013) investigated with MEG the coherence among SMA and motor area, during resting state and during isometric muscular contraction, before and after levodopa intake. Interestingly, they found an increased SMA–M1 coherence in OFF, during isometric contraction, that was remedied by levodopa. Nevertheless, coherence strength did not differ after intake of levodopa in resting state, suggesting that SMA–M1 coherence is particularly related to movement execution.

The second interesting trend appearing from our study is that, when considering the whole brain outflow, the only regions showing a strong tendency to change their connectivity were the ones belonging to the DMN. The importance of this network in patient with PD has been discussed above; particularly, it seems that dopaminergic therapy has a specific effect on both the DMN integrity and task-related brain activations in cognitively unimpaired PD patients, and that these effects seem to be dose-dependent (Krajcovicova, Mikl et al. 2012). However we have to consider that patients were acquired while in resting state, and that in this condition the DMN is the most active network of the brain. For this reason, the change in FC among these structures could represent a statistical bias.

METHODOLOGICAL CONSIDERATIONS

Beside the pathophysiological explanation for the absence of significant PDC findings in our study, we have to mention the possible role of the method limitations. Recording the

EEG in the MRI induces severe artifacts in the EEG. Indeed the quality of the EEG within the scanner is reduced compared to the EEG outside, because of the presence of conducting electrodes and wires within the static magnetic field itself. Several factors are involved in this quality impairment, such as small movements of the electrode wires caused by subtle head movements or vibrations of the scanner (Gotman, Kobayashi et al. 2006). The most important artifact that affects the EEG inside the scanner is the gradient artifact, whose amplitude is of the order of 50 times the background EEG. In order to remove it, the most widely used method consists of estimating the artifact and subtracting it from each frame (Allen, Josephs et al. 2000). By calculating the frequency removed by the gradient artifact corrections, we obtain a frequency inside the beta band, which will be for this reason removed from the analysis. Furthermore, by removing the cardioballistic artifact through Independent Component Analysis, the risk of removing independent components of signal, which are actually coming from the brain, cannot be excluded. To eliminate this hypothesis it will be necessary to perform the analyses on the EEG cleaned only for the gradient artifact. The influence of the removal of MRI gradient and ECG artifacts on multivariate measures among EEG signals, such as PDC (and other brain connectivity measures) is still unknown. Further exploration of these effects in different subject groups, using varying acquisition protocols and scanning equipment, should be performed to evaluate the sensitivity of the methods to these artifacts.

It is worthy to consider that, when comparing the differences in FC in the ON phase vs. the OFF phase, we observe a simultaneous increased BOLD-FC and a decreased EEG-FC. The electrophysiological substrate of spontaneous BOLD fluctuations constituting the basis of FC is still largely unknown. Very few studies come from implanted patients with epilepsy that not respond to medical treatment. Bettus et al. (Bettus, Ranjeva et al. 2011) studied the electrophysiological correlates of BOLD signal fluctuations in structures exhibiting

epileptiform discharges, by measuring in different session, correlations between intracerebral EEG and resting-state fMRI in five patients with temporal lobe epilepsy. They found an increase in connectivity measured from the intracerebral EEG but a decrease of connectivity measured from the BOLD signal in regions with epileptiform abnormalities relative to non-affected areas. This discrepancy, present also in our study, obtained by measuring connectivity of two signals of different nature (electrical and hemodynamic), demonstrates the challenge of interpreting connectivity changes. It could also suggest an alteration of neurovascular coupling in chronic diseases, such as temporal lobe epilepsy and PD.

The lack of statistical significance on the EEG-FC analysis could arise from the small sample of the studied population; the fact that the significance is present in the BOLD-FC analyses and not in the EEG-FC could be linked to the different statistical power of the two different analyses methods, as well as to the small number of the recording electrodes. Nevertheless this is a pilot study performed by advanced acquisition methods and sophisticated analysis in a homogeneous population. Further acquisition with a 128-or 256-electrodes EEG on largest sample populations should be performed to better explore the real limits and / or advantages of this technique on this field.

5. APPENDIX

EEG-fMRI was learned by Dr. Pittau during a fellowship of almost 3 years (2009-2011) at the Montreal Neurological Institute (McGill University, Canada), with the supervision of Prof. Jean Gotman. The development of EEG-fMRI at UNIBO has been done, starting from January 2012, with our own hardware and software and with the continue consultation and support with the Montreal Neurological Institute, which is an internationally recognized and specialized centre on this technique. Different steps were necessary:

1. **MRI compatible EEG setting**: EEG system that is able to acquire electric signal inside the MRI. BrainVision 2.0 (Brain Products, solution for neurophysiological research, Germany), software for recording and analyzing this type of signal, was installed. All Brain products have a CE certification. They are: a. BrainCap ; b. BrainAmp MR ; c. Brainvision Recorder ; d. Brainvision Analyzer.

    a. **"BrainCap".** EEG electrodes are usually metallic and therefore it is possible that the rapidly changing magnetic fields associated with scanning will induce a current which could lead to heating and localized burns to the patient's scalp. It has been shown that using nonferrous electrodes and leads and avoiding current loops involving the patient, result in safe recordings. "BrainCap" is a cap where there are 32/64 a-magnetic electrodes made with Ag or Ag-Cl. They have circular shape and a "hole" where conducting paste is placed. They are placed in plastic supports: this allows a good adhesion between the electrode and the scalp. The coils of the electrodes are collected in the vertex area of the patient to avoid loops.

    b. **"BrainAmp MR"** is a compact and screened amplifier, a-magnetic. It is battery powered. It has been projected to be placed inside the room with the magnet, behind the head of the patient. The short length of the coils used to connect the electrode with the amplifier is consistent with the safety requirement for the patient.

Neurophysiological signals are amplified at the head of the detector. They are converted in digital signals and are connected to a recording computer outside of the scanner room via an optic fiber cable. The optic cable ensures the absence of an electrically conductive bridge between the outside and the inside of the scanner room, which would break the magnetic shielding of the scanner room and deteriorate the quality of MR images.

c. **"BrainVision Recorder"** is multifunctional recording software designed to provide a platform for recording setup and execution. It allows settling the parameters necessary for the acquisition: the hardware filters on a channel by channel basis, channel by channel impedance, sampling rate of recordings, filters. The acquired data can be displayed in multiple ways and with different montages (original, bipolar and average). Each electrode is placed following the 10-20 system and its impedance value is displayed with a fully selectable color coding. The acquisition parameters as well as the impedance check are automatically stored and can be consulted anytime during the fMRI acquisition.

d. **"Brainvision Analyzer"** is a software that includes all necessary pre-processing functions, enhanced time-frequency analysis options, ICA, LORETA, MRI correction as well as a direct interface to MATLAB.

We have firstly acquired EEG data in 8 healthy control subjects *outside the MRI* to verify the quality of the EEG recordings: our expert electroencephalographers confirm that the quality of this system is as the same level as our standard usual acquisition method.

2. **EEG-fMRI acquisition and pre-processing**

After the approval of the local Ethic Committee, we have started to test the quality of the EEG-fMRI acquisition and analysis on a population of healthy control subjects. This step was

necessary to verify if the implementation of our method of acquisition and analysis was correct. To arrive to this conclusion we studied if the BOLD changes related to alpha rhythm triggered by eyes closure, was concordant with the previous data of literature. We decided to study the alpha rhythm because it is a physiological well detectable rhythm in healthy control subjects. The occipital BOLD de-activations were in agreement with previous studies in literature (Tyvaert, Levan et al. 2008).

Appendix figure 1: first subject with an EEG recorded inside MRI at UNIBO

EEG. We settled the parameters of Brain Vision Analyzer to remove the gradient artifacts and the cardioballistic artifacts from some EEG acquired inside the scanner during EEG-fMRI acquisitions.

a. **Gradient artifact removal**

The idea behind MRI artifact correction is that the gradient artifacts, that shows little or no variation, should be easy to detect and eliminate from any other ongoing and variable dataset such as the ongoing spontaneous EEG activity. Because it shows little or no variation, it is

possible to average all such artifacts and subtract the average from all the traces. The steps are the following:

i) Segmentation: we select the runs we want to analyze; we mark each of them with a "start" and "end" through the "Marker edit mode" option. Then we segment each of these runs so that we have many single files.

ii) MRI Artifact Correction: this option allows us to remove the gradient artifact from each single file (*Appendix figure 2*). We have to give the program the TR of the acquisition and the number of volumes acquired during one run. The program builds a "template" with the shape of the gradient artifact that does not change in time and then subtract it from the dataset.

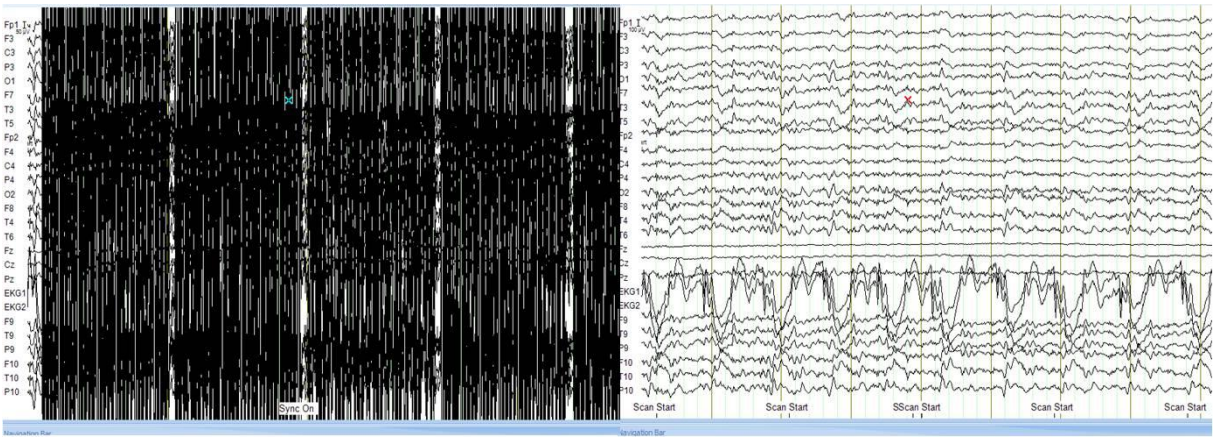

Appendix figure 2: removal of gradient artifact

b. **Cardioballistic artifacts removal**

i) Cardioballistic Pulse detection: In order to correct these artifacts, we have to first identify our R-Waves or at least some temporally stable and non changing point along our EKG episode and then perform the same type of template building and -subtraction that was used to correct the gradient data (*Appendix figure 3*).

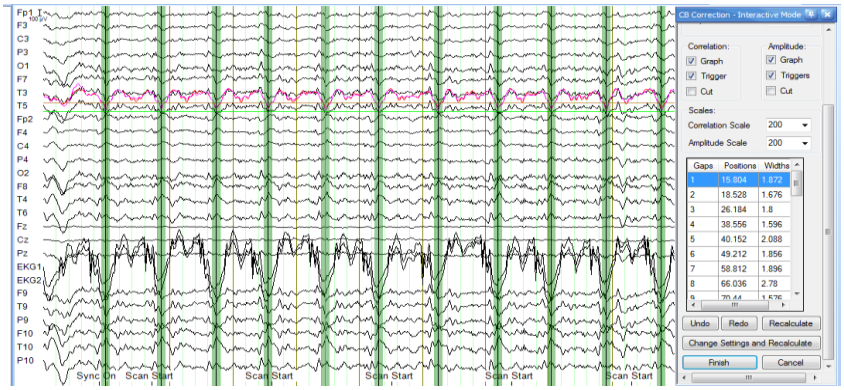

Appendix figure 3: detection of EKG peaks

ii) Correction of Pulse Artefacts: after marking, we can subtract the template built from the average of the previously marked EKG peaks (*Appendix figure 4*).

Appendix figure 4: removal of cardioballistic artifact

fMRI. At UNIBO the MR functional unit has experience with the software FSL which is a free, comprehensive library of analysis tools for FMRI, MRI and DTI brain imaging data created by the Analysis Group, FMRIB, Oxford, UK. In particular FEAT is part of FSL (FMRIB's Software Library) for model-based FMRI data analysis. The data modeling which FEAT uses is based on general linear modeling (GLM), otherwise known as multiple regression. It allows you to describe the experimental design; then a model is created that should fit the data, telling you where the brain has activated in response to the stimuli. In our case the model will be the timing of EEG events acquired by Brain Vision EEG.

6. REFERENCES

Allen, P. J., O. Josephs, et al. (2000). "A method for removing imaging artifact from continuous EEG recorded during functional MRI." Neuroimage **12**(2): 230-239.

Andres, F. G., T. Mima, et al. (1999). "Functional coupling of human cortical sensorimotor areas during bimanual skill acquisition." Brain **122 (Pt 5)**: 855-870.

Astolfi, L., F. Cincotti, et al. (2005). "Comparison of different multivariate methods for the estimation of cortical connectivity: simulations and applications to EEG data." Conf Proc IEEE Eng Med Biol Soc **5**: 4484-4487.

Beckmann, C. F., M. DeLuca, et al. (2005). "Investigations into resting-state connectivity using independent component analysis." Philos Trans R Soc Lond B Biol Sci **360**(1457): 1001-1013.

Bellec, P., P. Rosa-Neto, et al. (2010). "Multi-level bootstrap analysis of stable clusters in resting-state fMRI." Neuroimage **51**(3): 1126-1139.

Benar, C., Y. Aghakhani, et al. (2003). "Quality of EEG in simultaneous EEG-fMRI for epilepsy." Clin Neurophysiol **114**(3): 569-580.

Bettus, G., J. P. Ranjeva, et al. (2011). "Interictal functional connectivity of human epileptic networks assessed by intracerebral EEG and BOLD signal fluctuations." PLoS One **6**(5): e20071.

Birot, G., L. Spinelli, et al. (2014). "Head model and electrical source imaging: A study of 38 epileptic patients." Neuroimage Clin **5**: 77-83.

Biswal, B., F. Z. Yetkin, et al. (1995). "Functional connectivity in the motor cortex of resting human brain using echo-planar MRI." Magn Reson Med **34**(4): 537-541.

Biswal, B. B. (2012). "Resting state fMRI: a personal history." Neuroimage **62**(2): 938-944.

Brookes, M. J., M. Woolrich, et al. (2011). "Investigating the electrophysiological basis of resting state networks using magnetoencephalography." Proc Natl Acad Sci U S A **108**(40): 16783-16788.

Brown, P. (2003). "Oscillatory nature of human basal ganglia activity: relationship to the pathophysiology of Parkinson's disease." Mov Disord **18**(4): 357-363.

Brown, P. and C. D. Marsden (1999). "Bradykinesia and impairment of EEG desynchronization in Parkinson's disease." Mov Disord **14**(3): 423-429.

Brown, P., A. Oliviero, et al. (2001). "Dopamine dependency of oscillations between subthalamic nucleus and pallidum in Parkinson's disease." J Neurosci **21**(3): 1033-1038.

Buckner, R. L., J. R. Andrews-Hanna, et al. (2008). "The brain's default network: anatomy, function, and relevance to disease." Ann N Y Acad Sci **1124**: 1-38.

Bullmore, E. and O. Sporns (2009). "Complex brain networks: graph theoretical analysis of structural and functional systems." Nat Rev Neurosci **10**(3): 186-198.

Cassidy, M., P. Mazzone, et al. (2002). "Movement-related changes in synchronization in the human basal ganglia." Brain **125**(Pt 6): 1235-1246.

Cavanna, A. E. and M. R. Trimble (2006). "The precuneus: a review of its functional anatomy and behavioural correlates." Brain **129**(Pt 3): 564-583.

Centeno, M. and D. W. Carmichael (2014). "Network Connectivity in Epilepsy: Resting State fMRI and EEG-fMRI Contributions." Front Neurol **5**: 93.

Coito, A., G. Plomp, et al. (2015). "Dynamic directed interictal connectivity in left and right temporal lobe epilepsy." Epilepsia **56**(2): 207-217.

Cox, R. W. (1996). "AFNI: software for analysis and visualization of functional magnetic resonance neuroimages." Comput Biomed Res **29**(3): 162-173.

Damoiseaux, J. S., S. A. Rombouts, et al. (2006). "Consistent resting-state networks across healthy subjects." Proc Natl Acad Sci U S A **103**(37): 13848-13853.

Dansereau, C. L., P. Bellec, et al. (2014). "Detection of abnormal resting-state networks in individual patients suffering from focal epilepsy: an initial step toward individual connectivity assessment." Front Neurosci **8**: 419.

de Pasquale, F., S. Della Penna, et al. (2010). "Temporal dynamics of spontaneous MEG activity in brain networks." Proc Natl Acad Sci U S A **107**(13): 6040-6045.

de Rijk, M. C., C. Tzourio, et al. (1997). "Prevalence of parkinsonism and Parkinson's disease in Europe: the EUROPARKINSON Collaborative Study. European Community Concerted Action on the Epidemiology of Parkinson's disease." J Neurol Neurosurg Psychiatry **62**(1): 10-15.

De Vico Fallani, F., L. Astolfi, et al. (2010). "Large-scale cortical networks estimated from scalp EEG signals during performance of goal-directed motor tasks." Conf Proc IEEE Eng Med Biol Soc **2010**: 1738-1741.

Esposito, F., A. Tessitore, et al. (2013). "Rhythm-specific modulation of the sensorimotor network in drug-naive patients with Parkinson's disease by levodopa." Brain **136**(Pt 3): 710-725.

Fahoum, F., R. Zelmann, et al. (2013). "Epileptic discharges affect the default mode network--FMRI and intracerebral EEG evidence." PLoS One **8**(6): e68038.

Farmer, S. F. (1998). "Rhythmicity, synchronization and binding in human and primate motor systems." J Physiol **509 (Pt 1)**: 3-14.

Foffani, G., A. Priori, et al. (2003). "300-Hz subthalamic oscillations in Parkinson's disease." Brain **126**(Pt 10): 2153-2163.

Fox, M. D., M. Corbetta, et al. (2006). "Spontaneous neuronal activity distinguishes human dorsal and ventral attention systems." Proc Natl Acad Sci U S A **103**(26): 10046-10051.

Friston, K. J., L. Harrison, et al. (2003). "Dynamic causal modelling." Neuroimage **19**(4): 1273-1302.

Gelb, D. J., E. Oliver, et al. (1999). "Diagnostic criteria for Parkinson disease." Arch Neurol **56**(1): 33-39.

Gerloff, C., J. Richard, et al. (1998). "Functional coupling and regional activation of human cortical motor areas during simple, internally paced and externally paced finger movements." Brain **121 (Pt 8)**: 1513-1531.

Gotman, J., E. Kobayashi, et al. (2006). "Combining EEG and fMRI: a multimodal tool for epilepsy research." J Magn Reson Imaging **23**(6): 906-920.

Granger, C. W. J. (1969). "Investigating causal relations by econometric models and cross-spectral methods." Econometrica **37**: 424–438.

Grave de Peralta Menendez, R., M. M. Murray, et al. (2004). "Electrical neuroimaging based on biophysical constraints." Neuroimage **21**(2): 527-539.

Greicius, M. D., B. Krasnow, et al. (2003). "Functional connectivity in the resting brain: a network analysis of the default mode hypothesis." Proc Natl Acad Sci U S A **100**(1): 253-258.

He, B., Y. Dai, et al. (2011). "eConnectome: A MATLAB toolbox for mapping and imaging of brain functional connectivity." J Neurosci Methods **195**(2): 261-269.

Hughes, A. J., S. E. Daniel, et al. (1993). "A clinicopathologic study of 100 cases of Parkinson's disease." Arch Neurol **50**(2): 140-148.

Hurtado, J. M., C. M. Gray, et al. (1999). "Dynamics of tremor-related oscillations in the human globus pallidus: a single case study." Proc Natl Acad Sci U S A **96**(4): 1674-1679.

Jenkinson, M., C. F. Beckmann, et al. (2012). "Fsl." Neuroimage **62**(2): 782-790.

Keller, C. J., S. Bickel, et al. (2011). "Intrinsic functional architecture predicts electrically evoked responses in the human brain." Proc Natl Acad Sci U S A **108**(25): 10308-10313.

Krajcovicova, L., M. Mikl, et al. (2012). "The default mode network integrity in patients with Parkinson's disease is levodopa equivalent dose-dependent." J Neural Transm **119**(4): 443-454.

Lalo, E., S. Thobois, et al. (2008). "Patterns of bidirectional communication between cortex and basal ganglia during movement in patients with Parkinson disease." J Neurosci **28**(12): 3008-3016.

Lancaster, J. L., M. G. Woldorff, et al. (2000). "Automated Talairach atlas labels for functional brain mapping." Hum Brain Mapp **10**(3): 120-131.

Lemieux, L., J. Daunizeau, et al. (2011). "Concepts of connectivity and human epileptic activity." Front Syst Neurosci **5**: 12.

Leocani, L., C. Toro, et al. (1997). "Event-related coherence and event-related desynchronization/synchronization in the 10 Hz and 20 Hz EEG during self-paced movements." Electroencephalogr Clin Neurophysiol **104**(3): 199-206.

Levy, R., P. Ashby, et al. (2002). "Dependence of subthalamic nucleus oscillations on movement and dopamine in Parkinson's disease." Brain **125**(Pt 6): 1196-1209.
Levy, R., W. D. Hutchison, et al. (2000). "High-frequency synchronization of neuronal activity in the subthalamic nucleus of parkinsonian patients with limb tremor." J Neurosci **20**(20): 7766-7775.
Levy, R., W. D. Hutchison, et al. (2002). "Synchronized neuronal discharge in the basal ganglia of parkinsonian patients is limited to oscillatory activity." J Neurosci **22**(7): 2855-2861.
Litvak, V., A. Jha, et al. (2011). "Resting oscillatory cortico-subthalamic connectivity in patients with Parkinson's disease." Brain **134**(Pt 2): 359-374.
Logothetis, N. K. (2012). "Intracortical recordings and fMRI: an attempt to study operational modules and networks simultaneously." Neuroimage **62**(2): 962-969.
Louis, E. D., L. A. Klatka, et al. (1997). "Comparison of extrapyramidal features in 31 pathologically confirmed cases of diffuse Lewy body disease and 34 pathologically confirmed cases of Parkinson's disease." Neurology **48**(2): 376-380.
Maldjian, J. A., P. J. Laurienti, et al. (2003). "An automated method for neuroanatomic and cytoarchitectonic atlas-based interrogation of fMRI data sets." Neuroimage **19**(3): 1233-1239.
Marsden, C. D. and J. A. Obeso (1994). "The functions of the basal ganglia and the paradox of stereotaxic surgery in Parkinson's disease." Brain **117 (Pt 4)**: 877-897.
Marsden, J. F., K. J. Werhahn, et al. (2000). "Organization of cortical activities related to movement in humans." J Neurosci **20**(6): 2307-2314.
McKeown, M. J., S. Makeig, et al. (1998). "Analysis of fMRI data by blind separation into independent spatial components." Hum Brain Mapp **6**(3): 160-188.
Megevand, P., L. Spinelli, et al. (2014). "Electric source imaging of interictal activity accurately localises the seizure onset zone." J Neurol Neurosurg Psychiatry **85**(1): 38-43.
Michel, C. M., M. M. Murray, et al. (2004). "EEG source imaging." Clin Neurophysiol **115**(10): 2195-2222.
Obeso, J. A., M. C. Rodriguez, et al. (1997). "Basal ganglia pathophysiology. A critical review." Adv Neurol **74**: 3-18.
Ogawa, S., D. W. Tank, et al. (1992). "Intrinsic signal changes accompanying sensory stimulation: functional brain mapping with magnetic resonance imaging." Proc Natl Acad Sci U S A **89**(13): 5951-5955.
Ohara, S., T. Mima, et al. (2001). "Increased synchronization of cortical oscillatory activities between human supplementary motor and primary sensorimotor areas during voluntary movements." J Neurosci **21**(23): 9377-9386.
Plomp, G., C. Quairiaux, et al. (2014). "The physiological plausibility of time-varying Granger-causal modeling: Normalization and weighting by spectral power." Neuroimage **97C**: 206-216.
Pollok, B., D. Kamp, et al. (2013). "Increased SMA-M1 coherence in Parkinson's disease - Pathophysiology or compensation?" Exp Neurol **247**: 178-181.
Priori, A., G. Foffani, et al. (2002). "Movement-related modulation of neural activity in human basal ganglia and its L-DOPA dependency: recordings from deep brain stimulation electrodes in patients with Parkinson's disease." Neurol Sci **23 Suppl 2**: S101-102.
Raichle, M. E., A. M. MacLeod, et al. (2001). "A default mode of brain function." Proc Natl Acad Sci U S A **98**(2): 676-682.
Rowe, J., K. E. Stephan, et al. (2002). "Attention to action in Parkinson's disease: impaired effective connectivity among frontal cortical regions." Brain **125**(Pt 2): 276-289.
Schelter, B., J. Timmer, et al. (2009). "Assessing the strength of directed influences among neural signals using renormalized partial directed coherence." J Neurosci Methods **179**(1): 121-130.
Serrien, D. J. and P. Brown (2002). "The functional role of interhemispheric synchronization in the control of bimanual timing tasks." Exp Brain Res **147**(2): 268-272.
Serrien, D. J. and P. Brown (2003). "The integration of cortical and behavioural dynamics during initial learning of a motor task." Eur J Neurosci **17**(5): 1098-1104.

Serrien, D. J., R. J. Fisher, et al. (2003). "Transient increases of synchronized neural activity during movement preparation: influence of cognitive constraints." Exp Brain Res **153**(1): 27-34.
Shine, J. M., G. M. Halliday, et al. (2014). "The role of dysfunctional attentional control networks in visual misperceptions in Parkinson's disease." Hum Brain Mapp **35**(5): 2206-2219.
Shmuel, A. and D. A. Leopold (2008). "Neuronal correlates of spontaneous fluctuations in fMRI signals in monkey visual cortex: Implications for functional connectivity at rest." Hum Brain Mapp **29**(7): 751-761.
Silberstein, P., A. Pogosyan, et al. (2005). "Cortico-cortical coupling in Parkinson's disease and its modulation by therapy." Brain **128**(Pt 6): 1277-1291.
Smith, S. M., K. L. Miller, et al. (2011). "Network modelling methods for FMRI." Neuroimage **54**(2): 875-891.
Stefan, H. and F. H. Lopes da Silva (2013). "Epileptic neuronal networks: methods of identification and clinical relevance." Front Neurol **4**: 8.
Tessitore, A., M. Amboni, et al. (2012). "Resting-state brain connectivity in patients with Parkinson's disease and freezing of gait." Parkinsonism Relat Disord **18**(6): 781-787.
Tessitore, A., F. Esposito, et al. (2012). "Default-mode network connectivity in cognitively unimpaired patients with Parkinson disease." Neurology **79**(23): 2226-2232.
Tomarken, A. J. and N. G. Waller (2005). "Structural equation modeling: strengths, limitations, and misconceptions." Annu Rev Clin Psychol **1**: 31-65.
Tyvaert, L., P. Levan, et al. (2008). "Effects of fluctuating physiological rhythms during prolonged EEG-fMRI studies." Clin Neurophysiol **119**(12): 2762-2774.
Tzourio-Mazoyer, N., B. Landeau, et al. (2002). "Automated anatomical labeling of activations in SPM using a macroscopic anatomical parcellation of the MNI MRI single-subject brain." Neuroimage **15**(1): 273-289.
van Eimeren, T., O. Monchi, et al. (2009). "Dysfunction of the default mode network in Parkinson disease: a functional magnetic resonance imaging study." Arch Neurol **66**(7): 877-883.
Williams, D., M. Tijssen, et al. (2002). "Dopamine-dependent changes in the functional connectivity between basal ganglia and cerebral cortex in humans." Brain **125**(Pt 7): 1558-1569.